

Use of Eye Tracking Technology to Evaluate an UAV Operator's Attention Distribution during Training

Konstantin Metodiev¹, Zoya Hubenova¹, Liubomir Alexiev²

¹*Space Research and Technology Institute, Bulgarian Academy of Sciences*

²*Military Medical Academy, Bulgaria*

Corresponding Author: Konstantin Metodiev

ABSTRACT: The unmanned aerial vehicle working environment is highly dynamic and sets specific challenges and requirements for an operator to meet, such as to stay focused on refreshing flight situational awareness for long period of time. Operators are expected to quickly assess situations, choose control strategies, and make optimal decisions in a rapidly changing environment. The article hereby describes a pilot survey and analysis of eye tracking data related to studying peculiarities of correct distribution of UAV operator's visual attention over specific zones of interest within a flight simulator screen during training. The processed eye tracking data are augmented by flying and maneuvering quantities, gathered independently, and presented by tables and charts. Following a preliminary qualitative analysis, the obtained results show that all examinees manifest approximately identical fixations pattern throughout the flight, hence a clue to a trainee's proper attention distribution. Conclusions have been drawn from results of multiple measurements.

KEYWORDS UAV, eye tracking, human operator, visual attention, training, psychology

Date of Submission: 24-07-2021

Date of acceptance: 09-08-2021

I. INTRODUCTION

Currently, the Unmanned Aerial Vehicles (UAVs) are being applied to a rapidly growing number of areas, both military and civil, such as monitoring, forecasting, detection and assessment of damages in case of accidents, man-made disasters, state border patrol, transportation; monitoring of tall buildings and facilities, protection and control of critical energy infrastructure (power plants, main pipelines, dams, etc.), road traffic control, agriculture (control of crops, forests, etc.), industrial fishing, oceanography, signal retransmission, taking part in traffic management system, implementation of various scientific tasks, etc. From this perspective, training of UAV operators by means of virtual simulators appears to be a basis of professional skills formation in aircraft handling. It is obvious that the organization of personnel training in unmanned aerial systems (UAS), i.e., pilots-operators, payload operators, service specialists, etc., significantly affects safety levels and number of accidents, [1]. It is necessary for the operator to conform to common requirements developed in advance. Training centers and facilities should also satisfy identical criteria for certification in accordance with the international standards for UAV operators training [2].

The UAV working environment is very dynamic. It sets specific requirements for the operator to meet which is related to perception and processing a large amount of information. The operator is expected to quickly assess this information and respond accordingly depending on missions and tasks. At the same time, the operator either shares or exchanges information with other crew members. High level of responsibility and safety makes the operator's role even more complicated, forasmuch as UAV airborne could be interpreted as a possible threat to other aircraft or people.

Automation is an indisputable circumstance that contributes to increasing security and reliability of the flight mission. For example, contemporary unmanned systems differ significantly from each other in terms of degree of flight control automation: 1) joystick, pedals, and monitor with information from the UAV camera; 2) selection of desired parameters by the operator through an interface, and 3) full automation by autopilot after programming in advance. Two fundamental arguments, in favor of operator functions automation, are following: firstly, elimination of human error in high-risk operations and, secondly, reducing the operator's

workload and redirecting hers/his physical and mental resources to other activities. In all UAVs, the largest number of accidents occur during takeoff and landing. Today's main issues, concerning a trade-off between automation and man involved in UAV handling, include, but not limited to, following: interface design; workload; security system; crew selection; degree of automation.

Main purpose of the pilot study and related experiments is looking into operators' visual attention distribution, by means of eye tracking, during simulator-based training (section 3). Amount of data gathered by the eye tracker is quite sufficient as regards particular parameters required to carry out the presented research.

II. VISUAL ATTENTION AND EYE MOVEMENTS

Attention is officially defined as a mechanism that takes place in the brain to ensure that preferred input sensory information receives immediate cognitive processing before all other input data [3].

Visual attention is a complex conglomeration of processes which are activated by observing visual stimuli. It reflects not only the momentary perception of objects in the visual field, but also it appears to be an important element of cognitive activity related to other cognitive functions such as attention, working memory, vigilance, thinking, psychomotor coordination, orientation, planning, judgment and evaluation, decision making. An important condition for ensuring effective cognitive activity is correct distribution of attention, [1]. The attention is defined as an ability of the brain to respond adequately and simultaneously to various cognitive stimuli coming from the environment. This cognitive ability allows for parallel processing of information from different sources and successful completion of more than one task.

Many studies of visual attention have been conducted in the airplane cockpit. Some psychologists believe that there is not one set of resources for attention, but several. Even if there are multiple sets of resources, some researchers suggest that resources used for visual and auditory stimuli may not be completely separated from each other. This is more evident whenever the stimuli happen to occur at different locations [4]. In the cockpit, this could make a pilot unable to pay effective attention to both visual and auditory warnings coming from opposite sides of the cockpit.

Aviation psychologist Christopher Wickens [5] has proposed a theory of multiple attention resources, according to which each task has three dimensions that determine how attention is distributed. These dimensions are related to following questions:

- Which stage of cognitive processing does the task involve, for example, light perception or selection of a power switch?
- Does the task involve verbal or spatial processing, i.e., listening to communication or searching for a specific reading of an instrument?
- What are types of input and output involved – auditory or visual inputs; verbal or motor outputs?

Wickens' theory states that there may be a distinctive set of attention resources for each combination of the three dimensions of tasks, and that performance deteriorates if there is a shortage of these different resources.

In today's instrument-rich cockpits, pilots typically encounter more information (sensor inputs) exceeding what is possible to be processed outright, especially during emergencies where multiple warnings can flash and ring [6]. This can lead to a condition also known as a sensory overload. The sensory overload causes excessive shift in demand for cognitive resources. The theory of multiple sets of attention resources describes sensory overload as a trade-off between supply and demand that arises whenever trainee has to fulfill two or more tasks that require the same resource. Conversely, overload will not occur if multiple tasks do not require the same resources. Sensory overload has long been known to cause pilot error in simulator studies [7] and is thought to be a contributing factor to a number of aviation accidents due to pilot error. Sensory overload situations can cause disorientation, impair decision-making ability, either slow or stop an adequate response [8].

Experts in Human factor keep on studying attention related issues involving pilots, displays and instruments, and developing better guidelines for presenting information. Better guidance can help to reduce the potentially catastrophic effects of sensory overload and limiting ("tunneling") attention [9, 10].

Eye tracking is a process of measuring either the point of gaze (the very spot a person is looking at) or the eye ball angular movement relative to the head. An eye tracker is a device for measuring eye position and eye movement [11]. The device might be used to track eye line of sight to analyze the interaction of pilots with cockpit displays. Similar researches date back to the 1950s [12].

Eye movements give an idea of visual perception and visual information processing both of which largely affect the trainee's thought process. By measuring certain visual parameters, visual attention and quality of information perception can be assessed during different phases of the flight. It is also possible to estimate the UAV operator's particular condition, i.e., if she/he is adequate to address the current situation.

What is new is that, based on interpreting visual information obtained from screens, a question arises as to whether operators' training in perceiving and processing information is consistent with neurophysiology of the human eye. Pilots on board aircraft undergo training and acquire important habits in scanning visually the

environment outside and inside the cockpit. Particular attention is paid to object scan sequence and duration, with the sole aim at achieving automation in a normal environment and producing reflexes in extreme situations.

The UAV operator is largely deprived from a number of sensory stimuli necessary for perceiving the aircraft flying and maneuvering quantities. In most UAVs available today, especially higher-class ones, there is a sensory "hunger" due to lack of direct visual contact, no data arrive from sensors detecting spatial orientation (attitude) and position of the aircraft in a three-dimensional space, no sound and other stimuli are received revealing the UAV technical condition.

Information about the UAV condition is obtained through a complex interface displayed on a flat screen which in turn is an unnatural and an insufficient source of information regarding the rigid body dynamics. In order to interpret data from the screen, the operator is required a specialized training, specific qualities of neuropsychological perception of the environment. It is important to note that if stimuli are found where expected time required for perception and reaction decreases (a.k.a. preparation and accumulation of operator experience).

The UAV operators aim at perception, processing, and responding to a rapidly changing environment including a remotely controlled aircraft which justifies a preliminary scheme for data perception from environments with high information density. This, in turn, calls for prior theoretical and practical training as well as operator's experience increasing gradually.

III. MATERIALS AND METHODS

Participants. Ten volunteers, divided into two groups, have taken part in the pilot study. One group included 5 experienced UAV pilots while the other group included 5 volunteers with no or next to nothing experience. All participants had been shown the flight task they were expected to perform. After gaining confidence in airplane handling, the trainees successfully fulfilled prescribed tasks. All trainees had normal or corrected to normal visual acuity.

Yet another aim of the current study was to put the proposed methodology to a test so as to examine visual attention distribution of the UAV operators during training at simulators by means of an eye tracker. It was compulsory for the instructor to gather sufficient amount of data about all possible parameters recorded by the eye tracker and decide to accept those parameters of particular interest subsequently. It was also required to validate the experimental data taken by eye trackers through visualization and interpretation of the results. The usage of a desktop – based eye tracker is optional for it may be successfully replaced by a mobile one.



Fig. 1. C-Star simulator (SimLat, Inc.): pilot station equipped with Pupil Labs Core eye tracker

Experimental design. Studying operator's attention distribution on C-Star simulator, SimLat Ltd., Israel, [13], is a main goal of the current study. The experiment has been carried out at the pilot station which is equipped with 27 inches monitor, InterLink radio control module, mobile eye tracker Pupil Labs Core [14], Samsung Galaxy Tab S5e tablet used to gather raw data, Fig. 1, 2.



Fig. 2. Pupil Labs Core binocular headset: 1) World camera; 2) Nose clip; 3) NIR camera and IR LED @ 850 nm; 4) USB-C connector

Tasks and stimuli. Two tasks were to be performed in succession during the experiment:

Task 1. Generic (introductory) UAV flight in Palma de Mallorca Airport area including take-off, free flight within visibility zone, landing approach, landing. The general-purpose flight is a reconnaissance flight for trainee to acquire initial skills in handling the UAV control sticks. The weather conditions have been set as simple as possible. For training reasons, both take-off and landing procedures comply with relevant safety requirements.

Task 2. Performing a complicated flight task along the airfield traffic pattern. After taking-off, the trainee was said to follow traffic pattern designed in advance, Fig. 3. The flight route had been divided into three stages: take-off and climbing (blue), cruise (orange), landing approach and landing (yellow). It was obligatory for the trainee to maintain constant engine thrust (75%) and flight height (200 feet) wherever it is possible. Prior to rolling, the trainee must comply with a start check list.

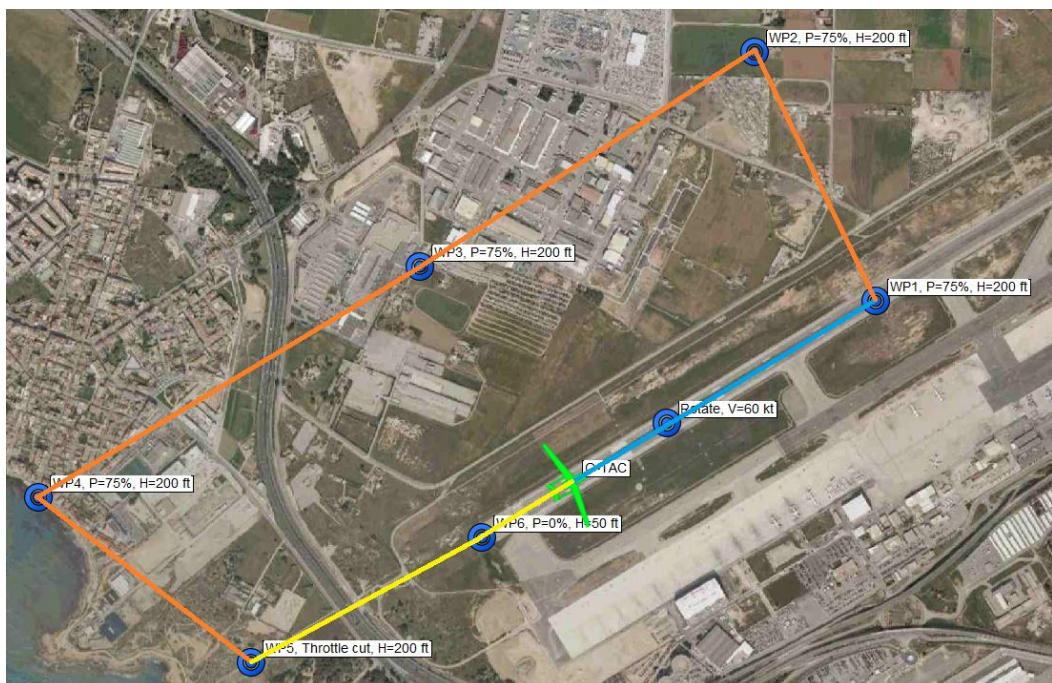


Fig. 3. Flight route stages

Last but not the least, the recommended distance between the trainee and the screen is 70-80 cm provided the world camera lens field of view is 120 deg. Prior to each flight, the instructor performs a calibration procedure.

After experiment, chosen data were extracted from the eye tracker recording. Data were synchronized in time with the simulator flight recorder and processed afterwards. To study visual attention distribution, following parameters were considered important: number and average duration of fixations within distinctive areas of interest and flight stages, saccades between fixations.

Prior to processing raw data, the pilot station screen had been formally divided into four zones of interest, Fig. 4, as follows: map (zone 1), video channel (zone 2), area containing main flight instruments such as artificial horizon, compass, altimeter, air speed indicator (zone 3), area containing auxiliary instruments (zone 4). Fixations were to be counted within each zone for each flight stage separately.



Fig. 4. Pilot station screen divided into four zones of interest

Counting fixations by regions of interest and flight stages. During the video recording stage, it is impossible for the mobile eye tracker user to refrain from moving much or at all. For this reason, objects appear with variable coordinates on the video stream. Aforementioned zones of interest are no exception to the rule; therefore, its limiting quadrant (region of interest) has to be measured continuously, frame by frame. One way to do so is to use four fiducial markers, for example either Aruco [15, 16] or AprilTag located in the region corners. These markers are also observable in Fig. 1. OpenCV library [17] provides for methods capable of recognizing markers and calculating their coordinates on the screen. After measuring coordinates the corners, the screen undergoes a perspective transformation closely resembling image cropping (cv::warpPerspective method). Whenever a key is pressed, the screen is stretched. Fig. 7 and 8 show identical screenshot taken prior to and after stretching. Exemplary Aruco markers used in the present study are shown in Fig. 5, id 105, 106, 107, 108, dictionary id 17.

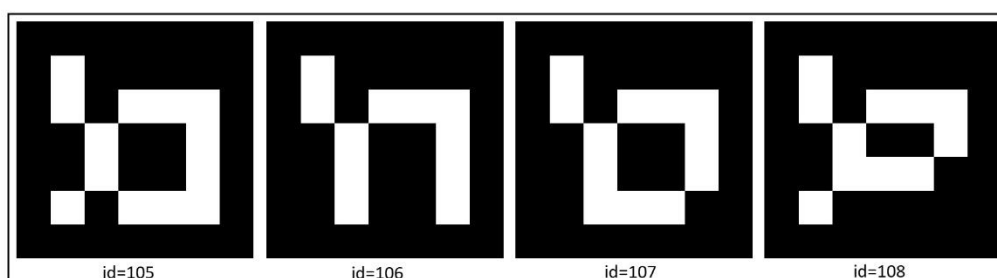


Fig. 5. Exemplary fiducial markers Aruco

Exemplary AprilTag markers, used in the current study in addition, are shown in Fig. 6, id 0, 14, 22, 17, dictionary id 36h11, [18].

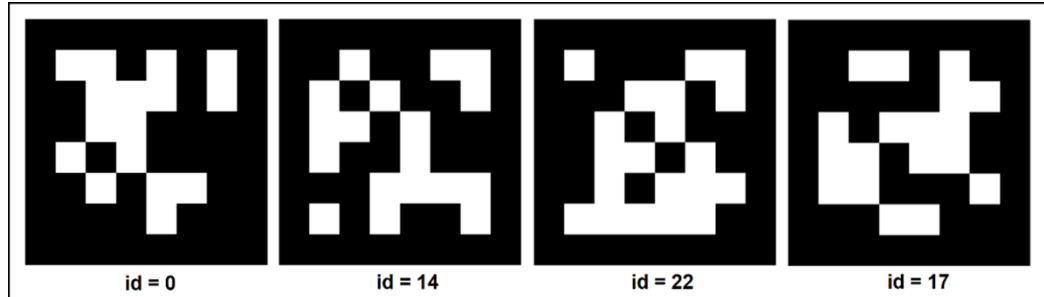


Fig. 6. Exemplary fiducial markers AprilTag

Fig. 7 shows a frame taken from the world camera of the mobile eye tracker. Four AprilTag fiducial markers are attached with sole purpose of measuring coordinates of the screen corners. OpenCV draws a green square around each marker indicating that the marker has been recognized by the cv::aruco::detectMarkers method. Only then can the geometric center of each marker (red dots) be calculated.

Fig. 8 shows the transformed region of interest for the same frame (cv::warpPerspective method). Following perspective transformation, that part of the image surrounding the region of interest (screen) is no longer available. The process resembles image cropping. What is more, spontaneous movements of the trainee's head are eliminated. The mobile eye tracker works like a desktop based one.

The method of perspective transformation (a.k.a. homography) makes it possible for the user to count fixations within each region of interest separately. The method advantages are following two:

- In the original image (general case), each zone of interest appears like an arbitrary quadrilateral. In the transformed image, the zones of interest are rectangles (Fig. 8, red frames). This makes it easier to determine whether the current fixation fits within a region of interest or not. It is only necessary for the user to make an elementary comparison between coordinates of the transformed fixation and the rectangle limits, i.e., transformed region of interest.
- During the process of eye tracking, the user is shaking head inevitably. Nevertheless, in the transformed image, the regions of interest remain stationary.

The method shortcoming is reduced resolution and poor quality of the transformed image which barely matters to the current study case.

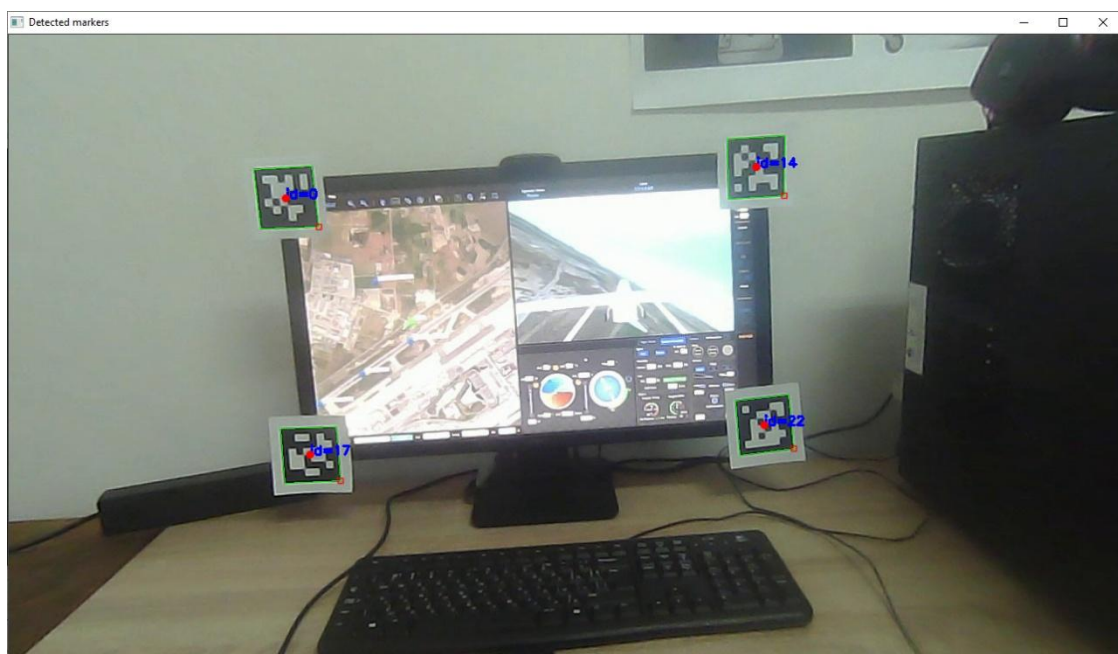


Fig. 7. C-Star pilot station with detected AprilTag markers and barrel distortion compensated



Fig. 8. Transformed region of interest with fixations being counted

Saccades distribution between zones of interest. The following exemplary table shows distribution of the saccades between distinct zones of interest. The table is filled as follows [19], Fig. 9. The row index (in green) shows zone of interest containing the current fixation location whilst the column index (in red) shows where the next fixation is located. The saccade should be recorded in a cell with indices corresponding to the position of initial and final fixations. For example, if the saccade starts at zone 1 (map) and ends at zone 2 (video channel), it should be counted in a cell with indices row 1 and column 2. The cells with equal indices (main diagonal of the matrix) are populated with saccades beginning and ending within a single zone of interest.

	1	2	3	4
1				
2		1		
3				
4				

Fig. 9. Saccade matrix pattern

Fig. 10 shows two successive fixations (color circles) and a saccade observable between them. The current fixation is colored in green while the fixation that follows is filled with red. The diameter of the circles depends on the fixation duration. The gaze starts from the green circle and moves towards the red one. The saccade shown starts in source 2 (video channel) and ends in source 1 (map). Therefore, the saccade must be recorded in cell with indices row 2 and column 1 in the table above (see arrows).

Pupil Player [20] provides for a plug-in for counting fixations by means of the Dispersion – Threshold Identification (I-DT) algorithm [21]. A shortcoming of the algorithm is inability to place gaze points found outside the current fixation in a particular class or group. In this way, it is impossible for the algorithm to identify a saccade.

Miscellanea. An important limiting condition should be mentioned. The C-Star simulator makes available for use an autopilot. Apart from executing autonomous flight, the autopilot is capable of stabilizing the airplane in one or more axes by actuating flight controls accordingly. In this way the airplane is unlikely to overturn. The stability augmentation system is what appears to be a damper attached to the pitch and roll axes. The yaw axis remains undamped. This makes it easier for a novice trainee to handle the UAV.

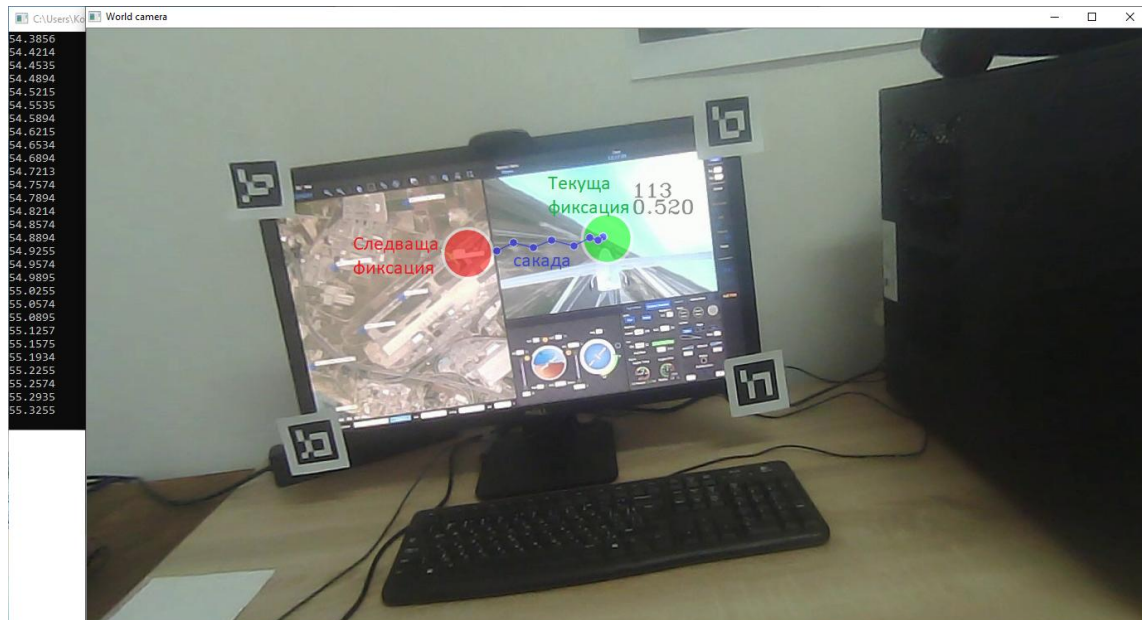


Fig. 10. Two consecutive fixations and a saccade between them

IV. RESULTS

The aim of the pilot study was to get opportunities that oculographic data analysis gives in relation to operators with different levels of training, thus reflecting the quality of visual attention and cognitive functions in performing identical tasks.

An important element of the flight task performance was development of an aircraft handling pattern. The UAV must follow these points in a certain predetermined direction, speed, and altitude. This is commonly known as airfield flight pattern. Seven such points were developed for the experiment purpose. The goal was to create a basic control pattern, unified for all trainees. The trainees had been selected according to predefined criteria, such as age, visual acuity, previous experience in handling UAV, etc. The trainee performed an introductory flight as well. In this way, each trainee got acquainted with the route and flight quantities required to be met at each flight point.

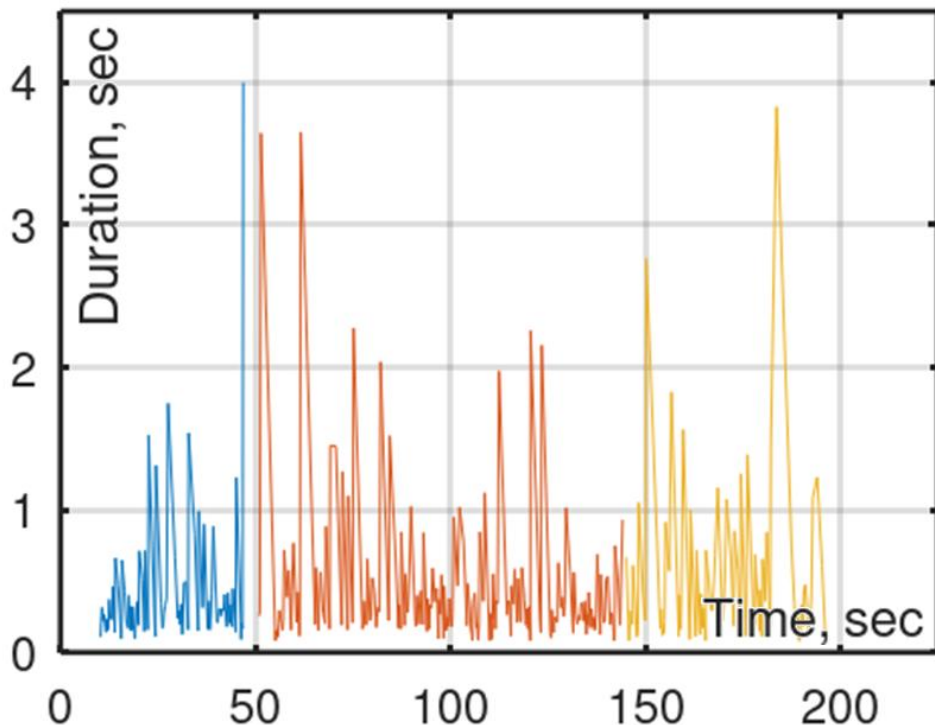
Skilled trainees fulfilled the flight task within 150 seconds on average. Little to no difference might be observed with regard to time to complete three flight stages under consideration, Fig. 3. At each check point along the route, trainees were able to meet specific requirements for throttle stick position, course, and altitude. Visual recordings were made throughout the flight displaying eye movement and marking visual attention distribution on the simulator screen, thus allowing to visualize the process of focusing and concentrating on certain areas of interest.

To better visualize data obtained from the eye tracker Pupil Labs Core, additional applications have been developed including generating a dynamic heat map and counting the fixations within each zone of interest separately. A C++ implementation of the OpenCV library has been used for this purpose, [18].

In Fig. 11 fixation durations, seconds, are shown in terms of flight time, seconds, for a *skillful* trainee. Different line colors correspond to different flight stages, shown in Fig. 3, as follows: take-off and climbing (blue), cruise (red), landing approach and landing (yellow). Fig. 9 does not display the way fixations are distributed within four zones of interest.

Tables 1 to 4 provide for different statistical data. Table 1 shows average number of fixations for each flight stage obtained from ten flights. Table 2 contains generic self-explanatory information about each flight stage. Table 3 contains data about number of fixations within zones of interest computed for each flight stages. Table 4 is almost identical to Table 3. The difference is that fixation durations are shown, not the number. In Fig 10, Tables 5 to 8, identical information is laid out for a *novice* trainee.

In both Fig. 11 and Fig. 12, extreme values of fixation durations (4000 ms) might be seen during the landing stage (yellow curves). The trainee is highly likely to be focusing on the video channel, zone 2, during landing. Same is confirmed by the figures in tables. During landing stage, the skillful trainee acquired 66 fixations in the video channel, Table 3, whilst the novice trainee got 46, Table 7. Regardless the difference, both values are the biggest as compared to the others in the same row (landing stage). Extreme values of the fixation durations might also be seen at the vicinity of first turn, i.e., end of stage 1.

**Fig. 11. Fixation distributions for an expert trainee****Table 1.** Average fixations number derived from 10 flight sessions

Zone 1, Map	Zone 2, Video	Zone 3, Artificial horizon and compass	Zone 4, Auxiliary sensors
130.40	147.50	122.40	5.2000

Table 2. Processed data

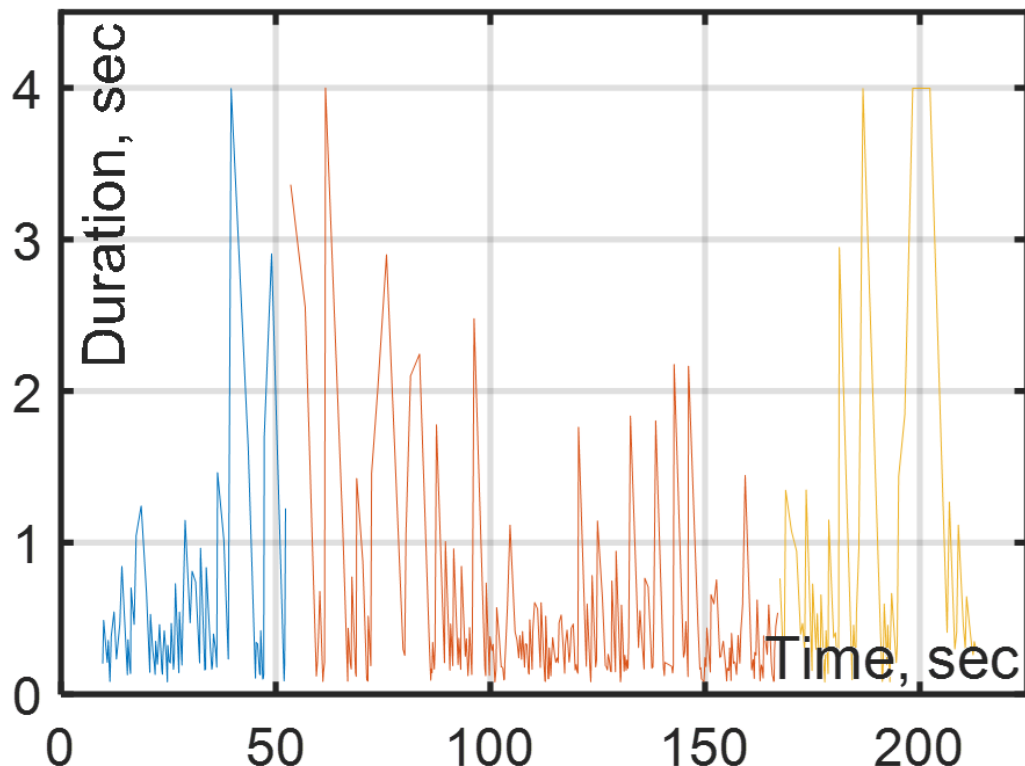
Stage / Parameter	Fixation's count	Fixations per second, s^{-1}	Average duration, ms	Standard error, ms	Total duration, s
Stage 1, from 9.98799 to 47.92 s	96	2.5308	402.2827	49.9806	38.6191
Stage 2, from 47.92 to 144.328 s	213	2.2094	416.8315	33.6062	88.7851
Stage 3, from 144.328 to 196.908 s	105	1.9970	465.8436	53.0490	48.9136

Table 3. Fixations distribution in terms of number

Stage \ Zone of interest	Zone 1, Map	Zone 2, Video	Zone 3, Artificial horizon and compass	Zone 4, Auxiliary sensors
Stage 1, from 9.98799 to 47.92 s	18	29	47	2
Stage 2, from 47.92 to 144.328 s	94	58	61	0
Stage 3, from 144.328 to 196.908 s	8	66	29	2
Total	120	153	137	4

Table 4. Fixations distribution in terms of duration, s

Stage \ Zone of interest	Zone 1, Map	Zone 2, Video	Zone 3, Artificial horizon and compass	Zone 4, Auxiliary sensors
Stage 1, from 9.98799 to 47.92 s	9.784	8.863	19.4841	0.488
Stage 2, from 47.92 to 144.328 s	40.263	14.743	33.779	0
Stage 3, from 144.328 to 196.908 s	1.809	32.598	14.21	0.296
Total	51.856	56.204	67.4731	0.784

**Fig. 12. Fixation distribution for a novice trainee****Table 5.** Average fixations number derived from 10 flight sessions

Zone 1, Map	Zone 2, Video	Zone 3, Artificial horizon and compass	Zone 4, Auxiliary sensors
111	181.5	59.3	3.4

Table 6. Processed data

Stage / Parameter	Fixation's count	Fixations per second, s^{-1}	Average duration, ms	Standard error, ms	Total duration, s
Stage 1, from 9.24805 to 53.4842 s	81	1.8311	496.1172	66.5989	40.717
Stage 2, from 53.4842 to 167.148 s	239	2.1027	440.7667	36.4667	105.344
Stage 3, from 167.148 to 213.529 s	64	1.3799	689.4593	110.0119	44.126

Table 7. Fixations distribution in terms of number

Stage \ Zone of interest	Zone 1, Map	Zone 2, Video	Zone 3, Artificial horizon and compass	Zone 4, Auxiliary sensors
Stage 1, from 9.24805 to 53.4842 s	9	40	28	4
Stage 2, from 53.4842 to 167.148 s	115	83	41	0
Stage 3, from 167.148 to 213.529 s	4	46	14	0
Total	128	169	83	4

Table 8. Fixations distribution in terms of duration, s

Stage \ Zone of interest	Zone 1, Map	Zone 2, Video	Zone 3, Artificial horizon and compass	Zone 4, Auxiliary sensors
Stage 1, from 9.24805 to 53.4842 s	4.191	16.910	18.2	1.416
Stage 2, from 53.4842 to 167.148 s	54.806	30.799	19.739	0
Stage 3, from 167.148 to 213.529 s	1.3940	38.808	3.9240	0
Total	60.391	86.5170	41.863	1.416

Table 9 shows saccades distribution between zones of interest at the pilot station in case of a novice trainee. Oddly enough, the 4th zone (auxiliary sensors) hasn't been observed at all which is the reason why cells in row 4 and column 4 are not populated. Excluding the matrix main diagonal, the biggest values might be found in cells with indices 2, 1 (49) and 1, 2 (44). Clearly, the pilot shifts her/his attention from the video channel to

the map and vice versa repeatedly. Given good weather conditions (i.e., natural horizon is considered discernible), it is sufficient for the trainee to be solely observing aforementioned zones in order to fulfil the flight task. The altimeter and the airspeed indicator (zone 3) are observed less frequently. In addition, the trainee's attention is shifted between adjacent zones such as map \leftrightarrow video, video \leftrightarrow artificial horizon, etc. It is less frequent for the trainee to shift attention along a diagonal on the screen as it might be seen in cells 3, 1 (1) and 1, 3 (5). A reference to the zones of interest numbering sequence is given in Fig. 4.

Table 9. Saccades between zones of interest

	1	2	3	4
1	44	44	5	
2	49	87	24	
3	1	33	43	
4				

In Fig. 13, a sigmoid fitted curve (logistic function) is shown modelling the eye ball rotation between two successive fixations, i.e., along a saccade. The curve model has been thoroughly discussed in paper [22]. In Fig. 14, first derivative to the sigmoid curve is shown indicating, in turn, the eye ball angular velocity. A non-linear least squares method was employed in order to minimize difference between measured and modelled data (blue dots in Fig. 13). In the current study case, the eye ball rotates within [0; 4] deg interval with maximum angular velocity of 140 deg/sec.

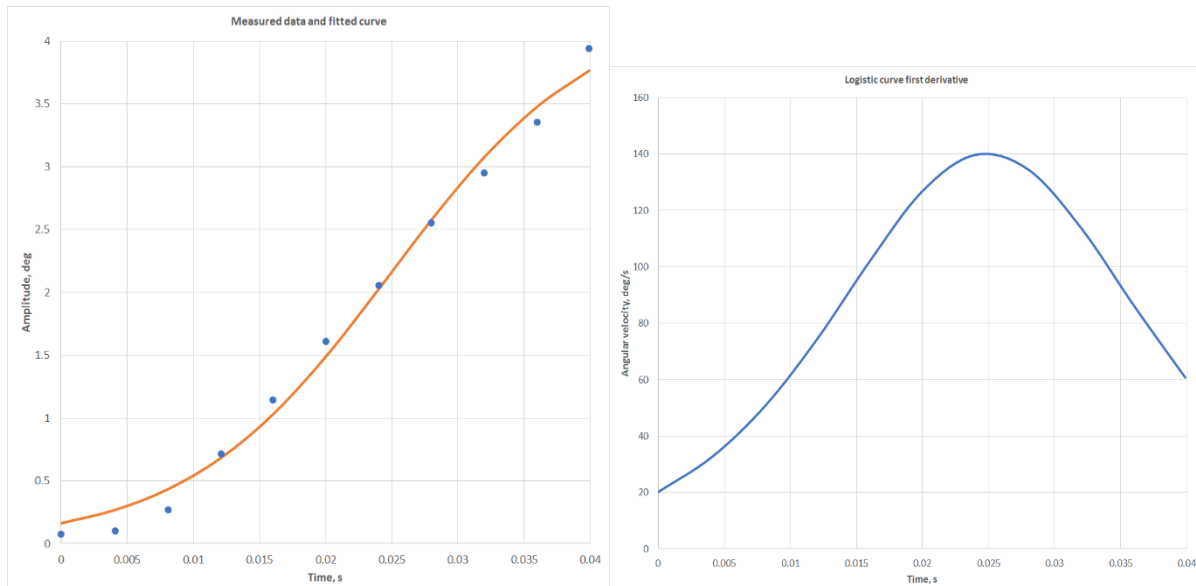
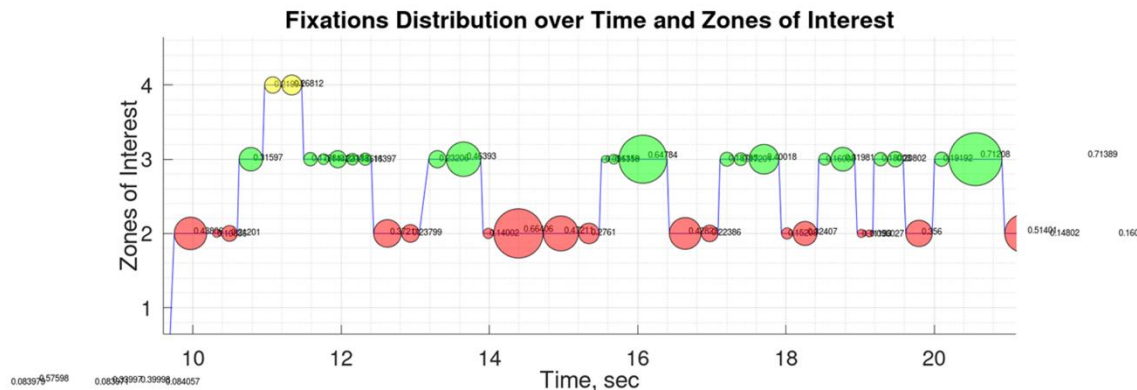


Fig. 13. Measured data and fitted curve

Fig. 14. First derivative of the fitted curve

In Fig. 15, time span of fixation distributions within zones of interest are shown [23]. Time is measured on the abscissa whilst zones of interest are plotted on the ordinate according to Fig. 4. Each fixation is represented by a circle. The bigger circle diameter, the longer duration. In Fig. 15, a small part of the chart is solely observable (about 10 seconds) due to limited space available. It shows the operator's fixation distributions shortly after starting take-off roll. The attention is switched between second and third zones only, i.e., the video channel and the airspeed indicator. Only after reaching V_1 speed (rotate) of 55 knots can the UAV lift off. Flight stages, according to what is depicted in Fig. 3, cannot be observed here unless information about stage time limits is accessible in advance.

By means of chart in Fig. 15, the instructor is able to find out whether the trainee makes critical errors in distributing her/his attention or not. In addition to flight data recorder (module PANEL, SimLat), the chart in Fig. 15 provides for a clue as to the nature of erroneous habits in UAV handling and how to proceed with training.



and “novice.” We also plan to expand our methodology based on the results of experiments conducted in real flights by means of UAVs at the test site.

ACKNOWLEDGEMENT

The current study has been funded by the Scientific Research Fund of the Republic of Bulgaria according to research contract No. KPI-06-H27/10, 11th of December, 2018.

REFERENCES

- [1]. Beier, S. Typeface Legibility: Towards Defining Familiarity. PhD Thesis. The Royal College of Art, London (2009).
- [2]. Crosby, M.E., Iding, M.K., and Chin, D.N. Visual search and background complexity: Does the forest hide the trees? Proc. UM 2001, Springer, p. 225-227 (2001).
- [3]. Willingham, D., Cognition: The Thinking Animal, 3rd edition, Prentice Hall, ISBN-13: 978-0131736887, ISBN-10: 0131736884 (1994).
- [4]. Driver, J., C. Spence, Spatial Synergies between Auditory and Visual Attention. In C. Umiltà & M. Moscovitch (Eds.), *Attention and performance 15: Conscious and nonconscious information processing*, pp. 311–331, The MIT Press (1994).
- [5]. Wickens, C.D. “Processing Resources in Attention, Dual Task Performance, and Workload Assessment.” In R. Parasuraman and R. Davies (editors), *Varieties of Attention*. New York: Academic Press (1984).
- [6]. Johnston, W., V. Dark, (1986). Selective attention. *Annual Review of Psychology*, 37, 43–75. <https://doi.org/10.1146/annurev.ps.37.020186.000355> (1986).
- [7]. Drinkwater, B., Performance of Civil Aviation Pilots under Conditions of Sensory Input Overload, *Aerospace Medicine*, 38(2):164-8 (1967).
- [8]. Harris, D. *Human Factors for Civil Flight Deck Design*. Hampshire, U.K.: Ashgate Publishing (2004)
- [9]. Dismukes, K., G. Young, R. Sumwalt, Cockpit Interruptions and Distractions: Effective management requires a careful balancing act. ASRS Directline, 10. Available: http://asrs.arc.nasa.gov/directline_issues/dl10_distract.htm (1998).
- [10]. Strayer, D., F. Drews, “Attention.” In *Handbook of Applied Cognition*. Druso, F.T. (editor). West Sussex, U.K.: John Wiley and Sons (2007)
- [11]. Duchowski, A., *Eye Tracking Methodology, Theory and Practice*, Second Edition, Springer Verlag, ISBN 978-1-84628-609-4 (2007).
- [12]. Fitts, P., R. Jones, J. Milton, Eye Movements of Aircraft Pilots during Instrument-Landing Approaches. *Aeronautical Engineering Review*, 9, 24–29 (1950).
- [13]. <https://www.simlat.com/products>
- [14]. Kassner, M., W. Patera, A. Bulling, Pupil: An Open-Source Platform for Pervasive Eye Tracking and Mobile Gaze-Based Interaction, Proceedings of the 2014 ACM international joint conference on pervasive and ubiquitous computing: Adjunct publication, pp. 1151–1160. New York: ACM. 2014, doi:10.1145/2638728.2641695 arXiv:1405.0006 (2014). <https://arxiv.org/pdf/1405.0006.pdf>
- [15]. Romero-Ramirez, F. J., R. Muñoz-Salinas, R. Medina-Carnicer, Speeded up Detection of Squared Fiducial Markers, *Image and Vision Computing*, vol 76, p.p. 38-47 (2018). https://www.researchgate.net/publication/325787310_Speeded_Up_Detection_of_Squared_Fiducial_Markers
- [16]. Garrido-Jurado, S., R. Muñoz Salinas, F. J. Madrid-Cuevas, R. Medina Carnicer, Generation of Fiducial Marker Dictionaries Using Mixed Integer Linear Programming, *Pattern Recognition*:51, 481-491 (2016). https://www.researchgate.net/publication/282426080_Generation_of_fiducial_marker_dictionaries_using_Mixed_Integer_Linear_Programming
- [17]. Bradski, G., The OpenCV Library, *Dr. Dobb's Journal of Software Tools* (2000) <https://opencv.org/>
- [18]. <https://github.com/samote4e>
- [19]. Goldberg, J. H., X. P. Kotval, Computer Interface Evaluation using Eye Movements: Methods and construct, *International Journal of Industrial Ergonomics* 24(6):631-645, October (1999).
- [20]. <https://docs.pupil-labs.com/core/software/pupil-player/>
- [21]. Salvucci, D., J. Goldberg, Identifying Fixations and Saccades in Eye-Tracking Protocols, *ETRA'00: Proceedings of the 2000 symposium on Eye tracking research & applications*, pp. 71–78, November (2000). <https://doi.org/10.1145/355017.355028>
- [22]. Metodiev, K., A Tool for Estimating Saccade Kinematics, Sixteenth International Scientific Conference “Space, Ecology, Safety 2020,” Sofia, Bulgaria, 4 – 6th of November (2020).
- [23]. Blascheck, T., K. Kurzhals, M. Raschke, M. Burch, D. Weiskopf, T. Ertl, State-of-the-Art of Visualization for Eye Tracking Data, *Eurographics Conference on Visualization EuroVis* (2014).
- [24]. Eaton, J. W., D. Bateman, S. Hauberg, R. Wehbring, *GNU Octave Version 6.3.0 Manual: A High-Level Interactive Language for Numerical Computations*, July (2021). <https://www.gnu.org/software/octave/index>

Konstantin Metodiev, et. al. "Use of Eye Tracking Technology to Evaluate an UAV Operator's Attention Distribution during Training." *American Journal of Engineering Research (AJER)*, vol. 10(8), 2021, pp. 145-157.